Pergamon

Journal of Structural Geology, Vol. 20, No. 2/3, pp. 135 to 148, 1998

0191-8141/98 \$19.00+0.00

PII: S0191-8141(97)00080-1

Brittle precursors of plastic deformation in a granite: an example from the Mont Blanc massif (Helvetic, western Alps)

A. GUERMANI and G. PENNACCHIONI

Dipartimento di Geologia, Paleontologia e Geofisica, Via Giotto 1, 35137 Padova, Italy

(*Received* 7 *January* 1997; *accepted in revised form* 18 *September* 1997)

Abstract—In the Mont Blanc Helvetic massif, granites record mesoscale Alpine structures, which include joints, veins, cataclastic to mylonitic shear zones and foliated granites. A detailed structural analysis indicates that brittle deformation predates plastic strain. Joints never pass through, and veins are offset by, cataclastic shear zones and mylonites. The mylonites progressively develop by plastic reactivation of cataclastic shear zones during greenschist facies metamorphic conditions. Plastic deformation is first localized in the brittle discontinuities and the fine-grained matrix of cataclasites. Then it involves the granite within brittle shear zones, and this is initially accomplished mainly by flow of reaction-softened aggregates of sericite, widely replacing the strain-supporting magmatic plagioclase. The brittle-to-plastic evolution has resulted in highly localized discontinuous plastic shear zones with high lateral continuity, and these characteristics are derived from reactivation of, and focusing along, pre-existing brittle discontinuities. In addition, mylonites may inherit high angles of intersection, and may contain granite porphyroclasts. These features may allow the inference of a precursor brittle deformation where the plastic overprint has completely erased the initial brittle fabrics. © 1998 Elsevier Science Ltd.

INTRODUCTION

Depending on the deformation mechanism, the way in which rocks deform may be classified as brittle or plastic (cf. Rutter, 1986). Brittle deformation involves cataclasis (microfracturing, movement along fractures, frictional grain-boundary sliding, and fragment rotation), while plastic deformation is mainly accomplished by dislocation motion and/or by diffusive mass transfer. A transition from brittle to plastic behaviour in rocks can be achieved by increasing the temperature, confining pressure and water content, or by decreasing the strain rate (e.g. Tullis and Yund, 1977, 1980). It is also, in a more complex way, dependent on the state of stress (Bürgmann and Pollard, 1994).

Plastic and brittle deformation structures are often associated in single exposures. In most cases, it can be demonstrated that brittle deformation is superimposed on the fabric produced during plastic flow, consistent with a retrograde exhumation path either during a continuous deformation under decreasing temperature or during different tectonic events (e.g. Watts and Williams, 1979; Gibson and Gray, 1985; Gaudemer and Tapponnier, 1987). Brittle and plastic structures may also be more or less coeval. Transient brittle instabilities during predominant plastic flow have been described, as for example the synmylonitic generation of pseudotachylytes close to the brittle–plastic transition (Sibson, 1977; Macaudiere and Brown, 1982; Passchier, 1982; Hobbs *et al.*, 1986; McNulty, 1995; Pennacchioni and Cesare, 1997). Bürgmann and Pollard (1994) reported both brittle and plastic fabrics on opposite sides of fault terminations, which they related to stress inhomogeneities around fault tips. The occurrence of veining episodes has been recognized over the whole metamorphic range where deformation is mainly plastic. In some cases, veins predate plastic deformation and several studies have emphasized the role of pre-existing brittle structures (veins) on nucleation and localization of plastic shear zones (Segall and Simpson, 1986; Gibson, 1990; Kronenberg *et al.*, 1990; Andersen *et al.*, 1991; Tobisch *et al.*, 1991; Boundy *et al.*, 1992; Früh-Green, 1994; Pennacchioni, 1996). Plastic deformation concentrated in veins has been related both to the geometric effect of introducing a mechanical anisotropy and to the catalysis of concomitant H_2O-rich fluid infiltration (e.g. Rubie, 1986). This suggests that precursor brittle episodes may play a fundamental role in nucleating plastic shear zones and in deformation partitioning under a wide range of conditions. This is especially true for coarse-grained rocks and rocks with large fractions of strong phases. These rocks exhibit high creep resistance and deform brittlely at the onset of deformation. The softening effect of grain-size reduction by cataclasis along a fault, allowing transition to prominent plastic deformation, has been microstructurally documented (e.g. Mitra, 1984; Goodwin and Wenk, 1995).

However, except for veins, only a few examples of macroscopic brittle-to-plastic deformation have been documented (Simpson, 1986; Goodwin and Wenk, 1995; Tourigny and Tremblay, 1997), and the importance of initial brittle structures in controlling subsequent plastic deformation is not fully understood. This is in part due to the fact that evidence of early brittle deformation is likely to be effectively erased during later plastic flow (Means, 1989; Tullis *et al.*, 1990) and in part to the fact that brittle structures have often been neglected in the study of metamorphic rocks. The latter stems from the assumption that these structures belonged to their late, low temperature uplift history. However, most metamorphic rocks are likely to have undergone a brittle-to-plastic structural evolution during prograde evolution. Understanding the influence of the brittle precursors may be relevant to the interpretation of the bulk deformation patterns. Thus, situations where deformation partitioning has preserved different steps of the brittle-to-plastic evolution are particularly worthy of inspection.

We present here a spectacular case of plastic shear zones overprinting and nucleating on pre-existing pervasive sets of cataclastic structures in granitic rocks in the Mont Blanc Helvetic massif (Western Alps, Italy). First, we provide field evidence from two sample areas that the association of brittle and plastic structures in the Mont Blanc granites results from a brittle-to-plastic evolution. Next, we use microstructural analysis to support the change in the deformation mechanism. Finally, we analyse those characteristics of plastic shear zones that may arise from a precursor brittle structural pattern.

GEOLOGICAL SETTING

The Mont Blanc 'external' massif is a Variscan basement unit belonging to the Helvetic domain of the Western Alps (Fig. 1a). It consists of paragneisses, migmatites and orthogneisses, intruded by a huge granitic body (Bonin *et al.*, 1993; von Raumer *et al.*, 1993). The granite intrusion has been dated at around 300 My (Baggio *et al.*, 1967; Bussy *et al.*, 1989). Intrusive contacts are only preserved in the southwestern part, whereas elsewhere the contact is tectonic.

The granitic body includes different rock types (Baggio, 1958; Marro, 1987): (1) coarse-grained to porphyritic granites, rich in centimetric K-feldspar; (2) medium-grained granites with less biotite and more quartz than the preceding type; and (3) biotite- and plagioclase-poor, fine-grained granites, relatively rich in aplitic dykes. Both (1) and (2) show a subvertical magmatic foliation striking NNE–SSW (von Raumer, 1967), which is consistent with the orientation of the aplitic dykes. Coarse-grained granites characterize the central sector of the granitic body, whereas medium-grained granites lie towards the borders. Fine-grained granites are widespread only in the southern part.

During the Tertiary, the Mont Blanc massif was affected by the Alpine orogeny and developed a non-pervasive greenschist facies metamorphic assemblage that consists, in granites, of quartz, albite, muscovite, biotite, chlorite, epidote and stilpnomelane (von Raumer, 1974; Borghi *et al.*, 1987). Rb/Sr dating of biotite yields ages in the ranges of 18–36 My (Baggio *et al.*, 1967).

Structural features

The Mont Blanc massif has often been represented as a stack of relatively rigid thrust sheets developed during NW (foreland)-vergent thrust tectonics (e.g. Escher *et al.*, 1993). Major deformation zones occur at the basal (NW) thrust, and at the NW and SE margins of the granite (Belliere, 1988). However, in the south, the massif is back-thrusted over the Mesozoic sedimentary rocks (Antoine *et al.*, 1975; Butler, 1985). Some authors described a fan-like arrangement of the SW–NE-striking structural planes, related to a pop-up structure of the Mont Blanc (Bertini *et al.*, 1985; Venera and von Raumer, 1995).

In some cases, the Mont Blanc granite has been reported as largely undeformed (e.g. Butler, 1985), but most studies indicate a diffuse deformation. In the southeastern part of the granitic body, Baggio (1958, 1964) and Baggio and Mezzacasa (1971) recognized foliated granites, cataclasites, mylonites and veins. Despite the detailed rock descriptions, the chronological relationships between the cataclasites and mylonites were not addressed. Bertini *et al.* (1985) described a fan-like arrangement of dip-slip fault planes in the granite, but give no detailed description of the faults themselves. Venera and von Raumer (1996) recognized a different spatial distribution of coeval plastic and brittle structures in the Mont Blanc granite, which they relate to a strain gradient and to different depths of deformation. From the NW to the SE, they described a transition from SE-dipping ultramylonites to *S–C* mylonites and NW-dipping cataclasites. However, they also reported cataclasites overprinting previously recrystallized fabrics.

In the Mont Blanc granite, the occurrence of hydrothermal veins, mainly of quartz and chlorite, is well known (von Raumer *et al.*, 1993 and references therein). They are mainly constituted by quartz and chlorite. Fluid inclusion studies on vein quartz (Poty *et al.*, 1974) indicate crystallization temperatures of around 400°C and pressures of 0.25–0.3 GPa. On the basis of radiometric ages [K/Ar and Rb/Sr on adularia and muscovite: Leutwein *et al.* (1970)] vein opening has been attributed to a late stage of the Alpine evolution (13–18 My).

So far, the relationship between these plastic (mylonites, gneissic foliation) and brittle (faults, cataclasites and veins) structures has not been investigated. Previous authors have often assumed that brittle structures belong to a late tectonic event (e.g. Belliere, 1988).

STRUCTURAL ANALYSIS

In the southeastern margin of the Mont Blanc granitic body, an area has been selected (Fig. 1b) to unravel the genetic and chronological relationships between brittle and plastic structures in the granite. A map of this area already existed (Baggio and Mezzacasa, 1971), and is redrawn slightly modified as Fig. 1(c). The original map of Baggio and Mezzacasa (1971) is very detailed. The only disagreement regards the inclusion between the high strain zones of N–S-trending structures, which were not

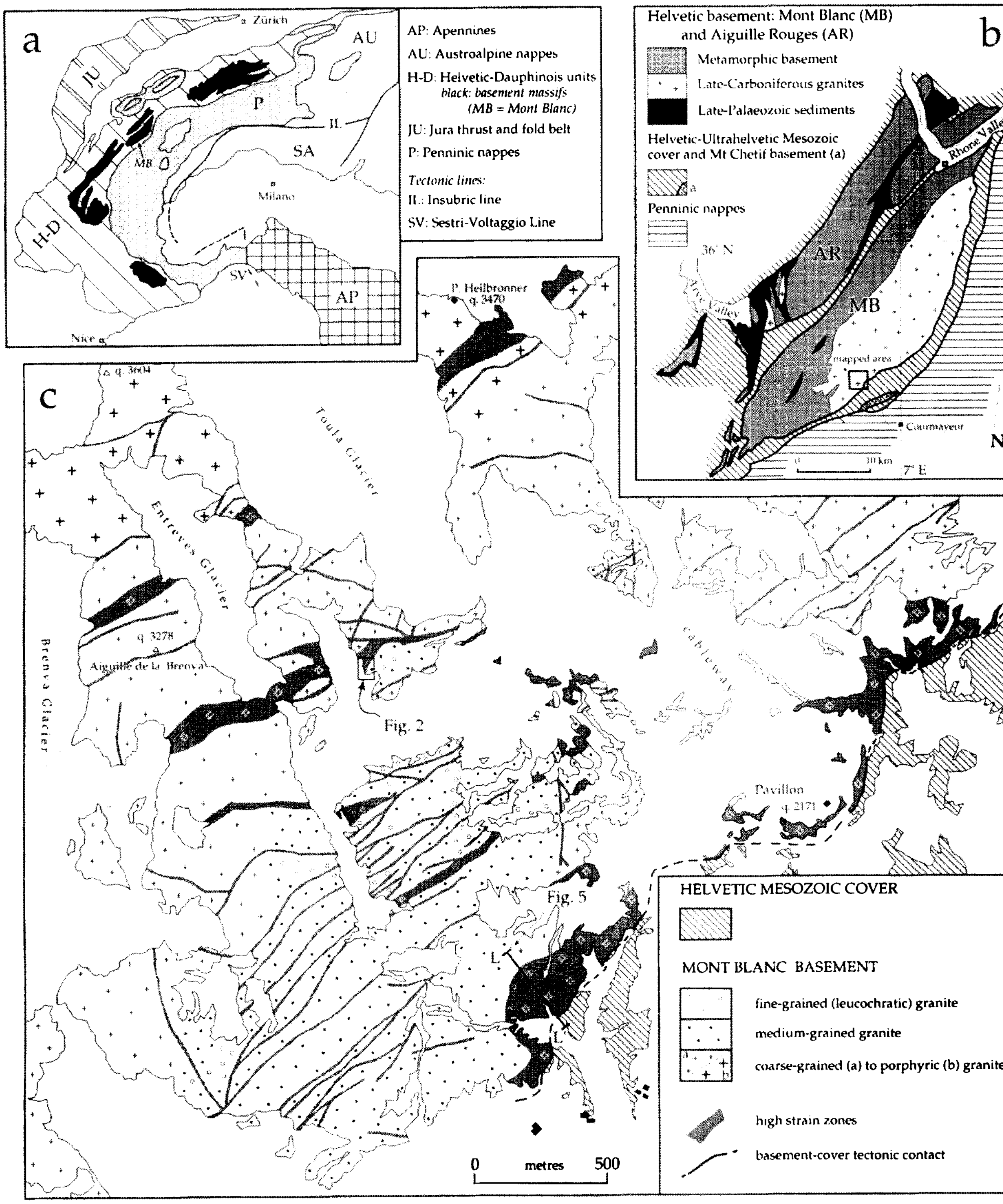

Fig. 1. (a) Tectonic sketch of the Alpine chain and location of the Mont Blanc massif. (b) Geologic sketch of the Mont Blanc–Aiguille Rouges Helvetic massifs. (c) Geological–structural map of the study area (redrawn and modified from Baggio and Mezzacasa, 1971). The mapped area is located on the southeastern side (Veny Valley) of the Mont Blanc granitic massif (see Fig. 1b). The box shows the location of the map area of Fig. 2, and L–L′ is the line of the section in Fig. 3.

recognized in the field and are therefore not reproduced in Fig. 1(c).

The whole granite is variably deformed throughout the area, with the strongly heterogeneous deformation concentrated into discrete (up to a few metres thick) brittle and plastic shear zones. The shear zones are characterized by great lateral continuity, and individual shear zones can sometimes be traced for hundreds of metres to kilometres. Shear zones are arranged roughly parallel to the SW–NE-striking contact between the granite and the sedimentary rocks. They also branch and converge to define an anastomosing pattern around lens-shaped low-strain domains.

At the map scale of Fig. 1(c), brittle and plastic shear zones cannot be distinguished because of their close association, and are represented collectively as 'high strain zones'. It should also be made clear that these high strain zones represent zones with a high density of mesoscale cataclasites and mylonites, in which the deformation is not, however, pervasive at the outcrop scale. In the same way, the intervening low strain domains do still commonly contain spaced, narrow mesoscale shear zones as well as completely undeformed granites.

Three major high strain zones can be recognized. The thickest one abuts the Mesozoic sedimentary rocks to the south. It is confined to the granite and does not affect the sedimentary rocks. The other two lie just south and north of the Aiguille de la Brenva (Fig. 1c).

Two sample areas have been chosen (see locations in Fig. 1c) to investigate and illustrate the structural evolution of the granite. The first area (Outcrop 1) is located near the front of the Toula Glacier at the lower margin of a major high strain zone and represents the transition between 'undeformed' and sheared granites. This glacier-polished outcrop, about 100 m^2, provides an excellent exposure of structures that would otherwise be easily obscured by weathering. In this outcrop, a detailed surface-map has been made (Fig. 2a). The second area (Outcrop 2) is a section of the major shear zone in contact with the Mesozoic sedimentary rocks (Fig. 3). This shear zone shows peculiar characteristics and provides further information on the structural evolution of the granite. Although the following observations mainly refer to the two sample areas, they are consistent with structural features occurring throughout the map area. The inferred structural evolution therefore may be considered as a model for the regional deformation.

Outcrop 1

Deformation involves a medium-grained granite with a weak N10°E-trending magmatic foliation. Joints, veins, shear zones and foliated granites can be recognized. On the basis of the distribution of the structures, two main domains can be distinguished. The southern part of the outcrop (domain 1) is characterized by mainly cataclastic, relatively spaced shear zones (Fig. 4a). These are located in undeformed granite, which includes frequent joints. In the northern part of the outcrop (domain 2), the shear zones are mainly mylonitic, foliated granites are present in low strain domains, and joints are absent (Fig. 4b).

Joints. In undeformed granite, joints occur in two roughly orthogonal sets that strike NNE–SSW and NW–SE, and dip steeply (J1 and J2 in Fig. 2b). In the field, joints appear as dark green, sharp planar surfaces outlined by thin ($\leq$1 mm) mica films. They are spaced in the range of 0.5–5 m away from the shear zones. Close to cataclasites, joints assume a curved shape, their spacing decreases and new joints appear at a lower angle to the shear zone boundary (see spot 1 of Fig. 2a). However, joints are confined to the granite and never cross cataclasites or mylonites (Fig. 4c, d).

Veins. Veins lie in both domain 1 and 2. In undeformed granites, two sets with a slightly different subhorizontal orientation (Fig. 2c), may be distinguished: (1) quartz–chlorite–adularia $\pm$ carbonate veins and (2) epidote veins. Vein infilling is influenced by composition of the host rock, and, in fine-grained granite, veins do not contain chlorite and epidote. Veins range from a few centimetres to several metres in length and from a few millimetres to decimetres in thickness; the largest veins are filled with quartz, chlorite and adularia. Veins are planar to sigmoidal and occur either isolated or arranged in an en échelon pattern. Mineral filling is both massive and fibrous. In wide veins, fibrous arrangements are present towards the vein tips, whereas the thickest parts include large idiomorphic quartz crystals (typical of growth in an open, fluid-filled cavity). Sometimes, veins are surrounded by haloes, up to some decimetres thick, where alteration of biotite causes bleaching of the granite.

Veins and joints show a strong geometric correlation. The J1 and J2 joint sets are orthogonal to the epidote and quartz–chlorite–adularia veins, respectively (compare Fig. 2b with Fig. 2c). In the undeformed granite, veins are also systematically oriented with respect to the shear zone boundaries. Their long dimension always lies in the shortening domain of the incremental strain ellipse consistent with the simple shear displacement of the cataclasites. In addition, sigmoidal veins and en échelon arrays indicate the same shear sense as the mylonites and cataclasites. Veins are offset by cataclastic shear zones (see spot 2 of Fig. 2a) and deformed by mylonites and never intrude them. Mylonitic shear zones commonly contain rows of quartz–feldspar lenses (Fig. 4c, d), wrapped around by the mylonitic foliation or contain quartz-rich layers, up to a few decimetres in thickness, transposed in the foliation. These lenses and layers are clearly derived from veins. Some lenses preserve relics of the primary vein texture due to deformation partitioning, and locally quartz-rich layers in the mylonites are still attached to undeformed veins in the country rock (Fig. 4e). Because of their initial orientation with respect to shear zones, veins underwent initial shortening and then stretching during progressive rotation toward the shear plane and are deformed into boudinaged folds in mylonites.

Shear zones. The outcrop shows a highly heterogeneous strain distribution due to the localization of deformation in discrete shear zones which have sharp boundaries with the host rock. High strain zones include

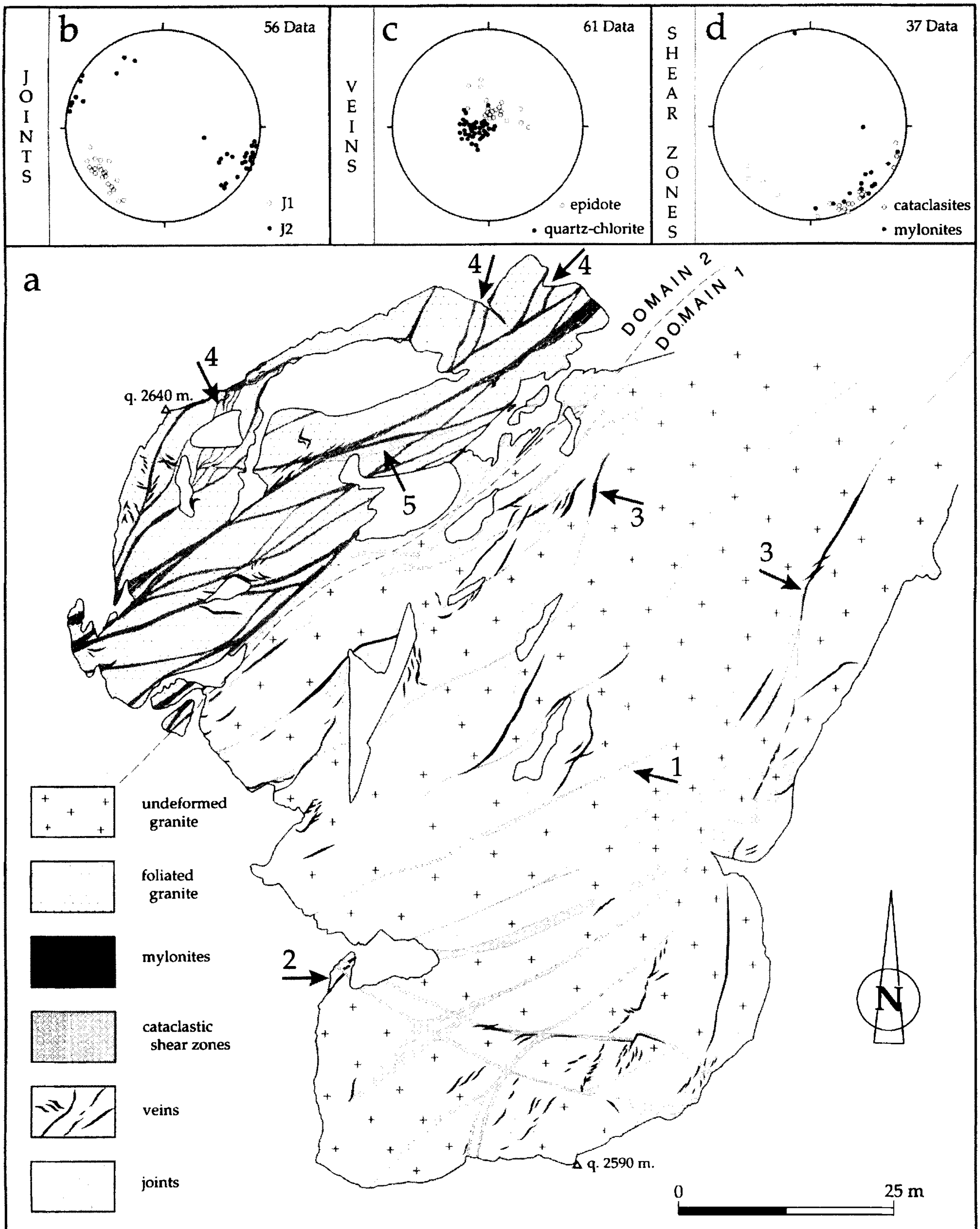

Fig. 2. (a) Surface map of the margin of a high strain zone. The location of the outcrop is shown in Fig. 1(c). The dashed line separates the low strain domain (1), in the south, where deformation is mainly recorded by brittle structures, from the high strain domain (2), where plastic fabrics dominate. Numbered arrows point to structures referred in the text. (b–d) Equal-area, lower-hemisphere stereographic projections of the mesoscopic fabric elements (poles).

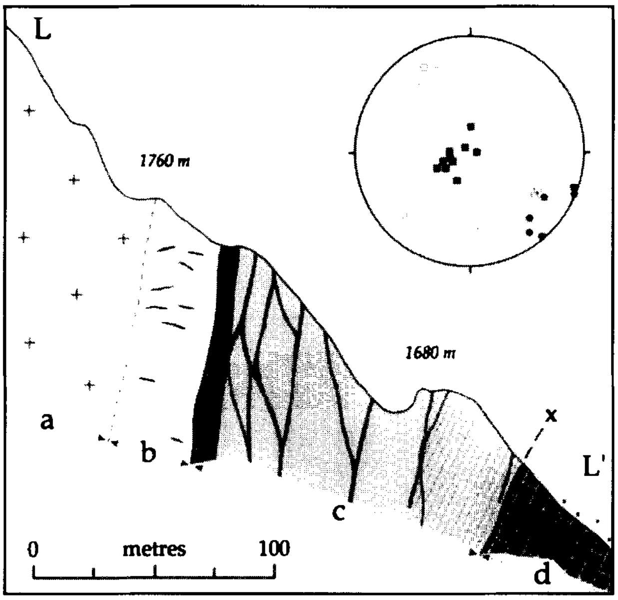

Fig. 3. Vertical cross-section across the major high strain zone in contact with the Mesozoic sediments (no vertical exaggeration). The location is shown in Fig. 1(c). From northwest to southeast, the following structural zones are distinguished: (a) undeformed granite; (b) granite with high density of joints and veins, (c) high strain zone and (d) Mesozoic sedimentary rocks. In (c), the main mylonitic horizons are distinguished (dark gray) inside more or less cataclased granites and fault rocks with varying degrees of plastic reactivation (light grey). Toward the contact with the sedimentary rocks, a dense mylonitic network appears (dashed overprint). In the equal area, lower hemisphere stereographic projection, the structural elements (poles) are: open circles, joints; filled squares, veins; filled circles, shear zones.

cataclasitic zones and mylonites. In both cases, kinematic indicators (marker offset, composite *S–C* fabric) give a dip-slip reverse movement, i.e. the displacement vector is roughly orthogonal to the surface of exposure in Fig. 2(a). Shear zones are mainly oriented around a NE–SW strike and dip steeply NW. When viewed in more detail, the shear zone array becomes complicated. In domain 1, a minor set of cataclasitic zones strikes ESE–WNW, dipping steeply toward NNE, and close to major veins cataclasites often merge in the vein plane (see spots 3 of Fig. 2a). In domain 2, mylonites show an anastomosing pattern around lozenged pods of foliated granite, and in three dimensions, they isolate disc-shaped domains. The angle between interfering shear zones is larger in domain 1 than in domain 2. Mylonites intersect commonly at angles less than 30°. However, domain 2 also contains shear zones in the foliated granites at higher angles to the bulk shear plane (see spots 4 of Fig. 2a), which may be higher than 80° in the case of some narrow (centimetre-thick) mylonites.

Although cataclasitic structures and mylonites prevail in domain 1 and domain 2, respectively, they occur in close association (Fig. 4c, d). In domain 1, the widest (1–3 m-thick) cataclastic bands are commonly rimmed by narrow (centimetre-thick) mylonite horizons, which are too thin to be represented in Fig. 2(a). Mylonites may occur on both or only one side of cataclasitic bands. However, in domain 2, mylonites sometimes include remnants of cataclastic granite at their margin (see spot 5 of Fig. 2a). However, cataclasitic shear zones always affect undeformed granites or veins, and never include clasts of mylonite or foliated granite, while mylonite layer may include lenses of cataclastic granite (Fig. 4d).

Cataclasitic shear zones. These are zones of concentrated fracturing (Fig. 5a), which only locally have evolved to matrix-dominated cataclasites and fault breccias. Narrow cataclastic bands develop initially as zones consisting of conjugate sets of en échelon, centimetre-spaced fractures (Fig. 5b), which subdivide the granite into blocky, rhomboidal elements. With increasing strain, fractures increase in density, and fracture planes become more irregular. This leads to a dense network with a statistically preferred orientation parallel to the boundary of the shear zone. Mica-filled fractures become thicker, and granite elements show relative displacements along these discrete fractures. Only locally have thin layers of cataclasites developed (Fig. 5c). The fracture-filling and cataclasite matrix is foliated, and a slickenside striation, parallel to the lineation in the mylonites, is visible on the fracture planes.

Mylonites. Mylonites form most of the shear zones in domain 2, but also occur in domain 1, associated with dominant cataclastic shear zones. They apper dark green to light green–grey and consist of fine-grained, thin-layered rocks with a strong foliation parallel to the shear zone boundary (Fig. 4b–e & 5d). The foliation plane contains a mineral stretching lineation consistent with approximately dip-slip movement. The transition to the country rocks is generally very sharp (discontinuous shear zones), and sigmoidal foliations are rare and limited to some small-scale examples. The thickness of mylonites is in the same range as that of the cataclastic shear zones.

Fig. 4. (a) Cataclastic shear zone across 'undeformed' granite consisting of several brittle planes converging to a main cataclastic fault. Hammer for scale. (b) Plastic shear zone at the contact between domain 1 and domain 2 (outcrop 1). Mylonites ultramylonites are in sharp contact with, and anastomose around, 'undeformed' granites showing a slight magmatic foliation (going from the bottom left towards the top right). Coin is shown for scale. (c) Joints abutting against a fault zone. Fault rocks include a cataclastic granite (cat), cross-cut by a network of thin discrete mylonite horizons, and well-foliated mylonites (myl). Note the quartz–adularia vein lens (arrow) inside the shear zone. Lens cap for scale. (d) Narrow brittle-plastic shear zone across jointed granite and interpretive sketch. Joints occur in different sets inclined at high and low angle to the shear zone boundary and do not cross the fault rocks. Inside the shear zones fault rocks include cataclasites (shaded in the sketch) and roughly to well foliated rocks (black). Thin horizons of mylonites wrap around a cataclasite pod in the centre of the photo and, on the right, cataclasites and mylonites surround a quartz–adularia vein lens (vertical lines). Lens cap shown for scale. (e) Quartz–adularia veins dragged into a mylonite. In the granite outside the shear zone, the orientation of the vein is consistent with the sinistral shear displacement in the mylonite, lying in the shortening domain of the instantaneous strain ellipse. Scale bar: 5 cm.

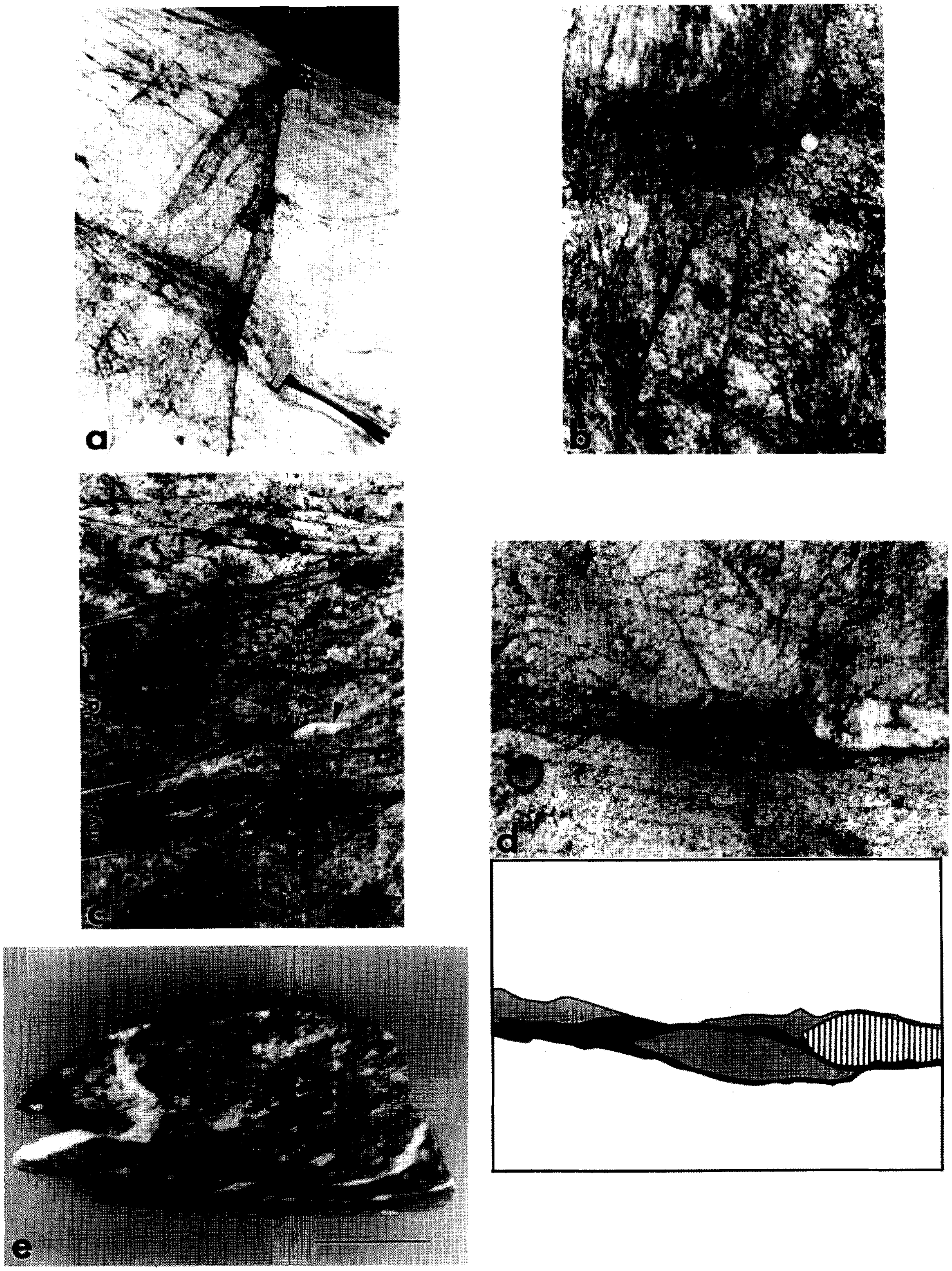

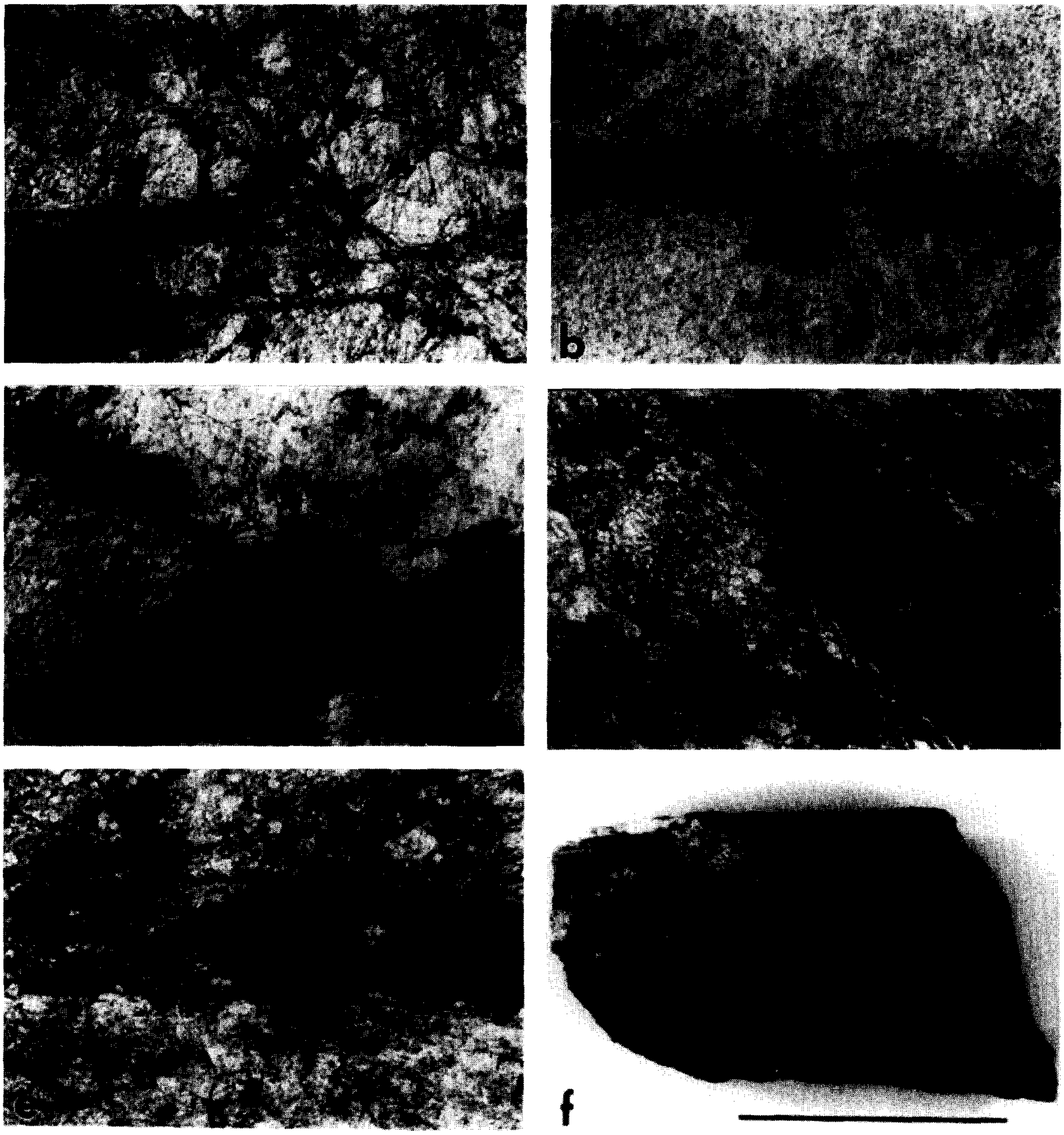

Fig. 5. (a) Interior of a cataclastic shear zone, characterized by a dense network of fractures. The shear zone boundary is approximately parallel to the base of the photo. Pen shown for scale. (b) Incipient brittle shear zone across undeformed granite defined by conjugate en échelon fracture sets. Lens cap shown for scale. (c) Thin layer of cataclasite with partial plastic overprint (note the foliation in the lower left) at the border of a cataclastic shear zone. In the granite (above the shear zone), low angle joints increase in density near the shear zone boundary, but do not cut across cataclasite–mylonite horizon. The white layer displaced by the shear zone is an aplitic dyke. Lens cap shown for scale. (d) Plastic structures in domain 2: ultramylonite (on the right) is in contact with foliated granites, which show a dense network of anastomosing microshear zones, resulting in an augen structure (eyes are slightly deformed granite). Note the white quartz–adularia lens (arrow) derived from a former vein. Pencil shown for scale. (e) Sharp contact between fractured granite (lower part) and a fault breccia (upper part). The breccia consists of angular clasts of granite embedded in a fine-grained, structureless dark matrix. Lens cap shown for scale. (f) Plastically deformed fault breccias showing rounded elements of granite, derived from former clasts, set in a foliated matrix; asymmetric biotite pressure shadows (arrows) are clearly visible around rock fragments. Scale bar: 5 cm.

Foliated granites. In domain 2, the domains between mylonites are occupied by foliated granites (orthogneisses) that display a rough foliation subparallel to the bounding mylonites, but largely preserve the magmatic mineral assemblages. Foliation is defined by discontinuous mica-rich layers, rows of microboudinaged K-feldspars and lenses of quartz. The transition from foliated granite to mylonites is often marked by a zone characterized by a network of anastomosing millimetric shear zones that gives the rock an augengneiss-like texture, where the 'augen' are granite domains (Fig. 5d).

Outcrop 2

The high strain zone at the granite-cover contact is about 200 m thick and affects medium- to fine-grained granites. The strongly deformed granites are in contact through a sharp fault plane with the underlying sedimentary rocks. A profile of the deformation zone along the Brenva stream is presented in Fig. 3. Deformation structures in granites within the high strain zone include both brittle and ductile fabrics as in outcrop 1. However, brittle deformation was stronger than in outcrop 1. Granites show a pervasive network of fractures or, as a result of diffuse microfracturing, they assume a dark appearance and, although the magmatic minerals are still recognizable, the magmatic texture is strongly disrupted. These rocks are cross-cut by centimetric to metric horizons of black, matrix-dominated cataclasites and fault breccias. Fault breccias consist of angular clasts of undeformed granite, reaching up to a decimetre in diameter, floating in a dark isotropic matrix (Fig. 5e). Mylonites are never included as clasts in fault breccias.

Brittle fabrics were overprinted to varying degrees by plastic deformation, and mylonitic horizons (up to a few metres wide) occur at different levels in the high strain zone. A zone of dominant mylonitic deformation and a dense network of mylonites are present at the upper and lower boundaries of the high strain zone, respectively. Superposition of plastic deformation over fault breccias gives rise to a foliated matrix and rounding of clasts and partially obliterates the breccia texture. The developing mylonites consist of a dark matrix of biotite and albite, which include porphyroclasts of granite surrounded by biotite-filled pressure shadows (Fig. 5f).

In the 'undeformed' granite outside the high strain zone, joints and veins are frequent and show similar orientation as in outcrop 1 (see stereonet in Fig. 3). Inside the high strain zone, quartz ($\pm$chlorite) veins are present showing an irregular orientation; they never cut across the mylonites.

MICROSTRUCTURES OF DEFORMED GRANITES

Compared to the field observations, the microstructural analysis provides evidence for an extensive microfracturing and alteration of granites, a pervasive recrystallization and plastic reactivation of brittle fabrics, and the presence of fluids during the brittle-to-plastic shear. Under the microscope, macroscopically undeformed granites show a pervasive network of grain-boundary and transgranular microfractures (Fig. 6a). Microfractures are filled with dominant quartz aggregates ($\pm$carbonate, chlorite, biotite II, albite and sericite), even where they cross-cut feldspars. The diffuse microfracturing of granite is stronger in outcrop 2 than in outcrop 1. This is correlatable with the different intensity of the macroscopic brittle deformation.

Notwithstanding the macroscopic appearance of brittle fabrics, the joints, the fracture network of cataclastic shear zones and cataclasites have undergone pervasive mineralization and recrystallization under greenschist facies metamorphic conditions and are involved in incipient to strong plastic deformation (Guermani, 1997). In the initial stages, plastic deformation is confined to the network of brittle discontinuities or to the fine-grained cataclastic matrix of fault rocks, but does not involve (or only slightly involves) the intervening granite or the granite clasts in fault breccias. Joints are filled with green–brown biotite, white mica and titanite, and the aggregate is often foliated parallel to the joint walls. Incipient cataclastic shear zones show three main sets of fractures, showing orientation maxima lying approximately parallel, at 45° and 135° to the shear zone boundary (Fig. 6b). The fractures have a different mineral filling depending on their orientation. One set of fractures inclined to the shear plane are dilational veins and are mainly filled by fine-grained quartz$\pm$biotite$\pm$white mica. In the other two fracture sets, the mineral filling consists mainly of white mica or white mica + biotite. The fracture system is commonly plastically reactivated to produce a composite discrete foliation network resembling a *S–C–C′* fabric. In the best preserved cataclasites and fault breccias (Fig. 6c), the matrix consists of fine-grained isotropic granoblastic aggregate including randomly oriented white mica. However, the matrix is commonly plastically deformed and well foliated, and the isotropic fabric only occurs locally in the regions shielded from deformation around granite clasts (Fig. 6d). Deformation partitioning around granite clasts produces white mica-rich domains, along high shear-strain domains, and biotite-rich pressure shadows. Rounded porphyroclasts of granite may survive up to very high strains and, in strongly foliated phyllonites, may record the original derivation from fault breccias.

The development of mylonites from cataclastic granites is accomplished by the progressive involvement in plastic deformation of the magmatic minerals, which combines with plastic reactivation of the brittle discontinuities and of the fine-grained cataclasite matrix. Initial plastic deformation of granite is enhanced in areas affected by the brittle deformation because of a strong greenschist facies alteration of granites. This is likely to be related to fluid advection along the brittle discontinuities. In the granites, the infiltration of fluids from fractures is allowed by the increased permeability related to the diffuse microfracturing. Mineral trasformations include replacement of magmatic plagioclase and biotite I by aggregates of sericite$\pm$epidote and by biotite II, respectively. These fine-grained reaction-softened aggregates flow easily into schistose elongated domains and layers that outline the foliation. Plagioclase is surrounded and/or dissected by discrete mica layers arranged into *S–C* geometries (Fig. 6e). In protomylonites, the magmatic quartz (quartz I) and the K-feldspar play only a minor

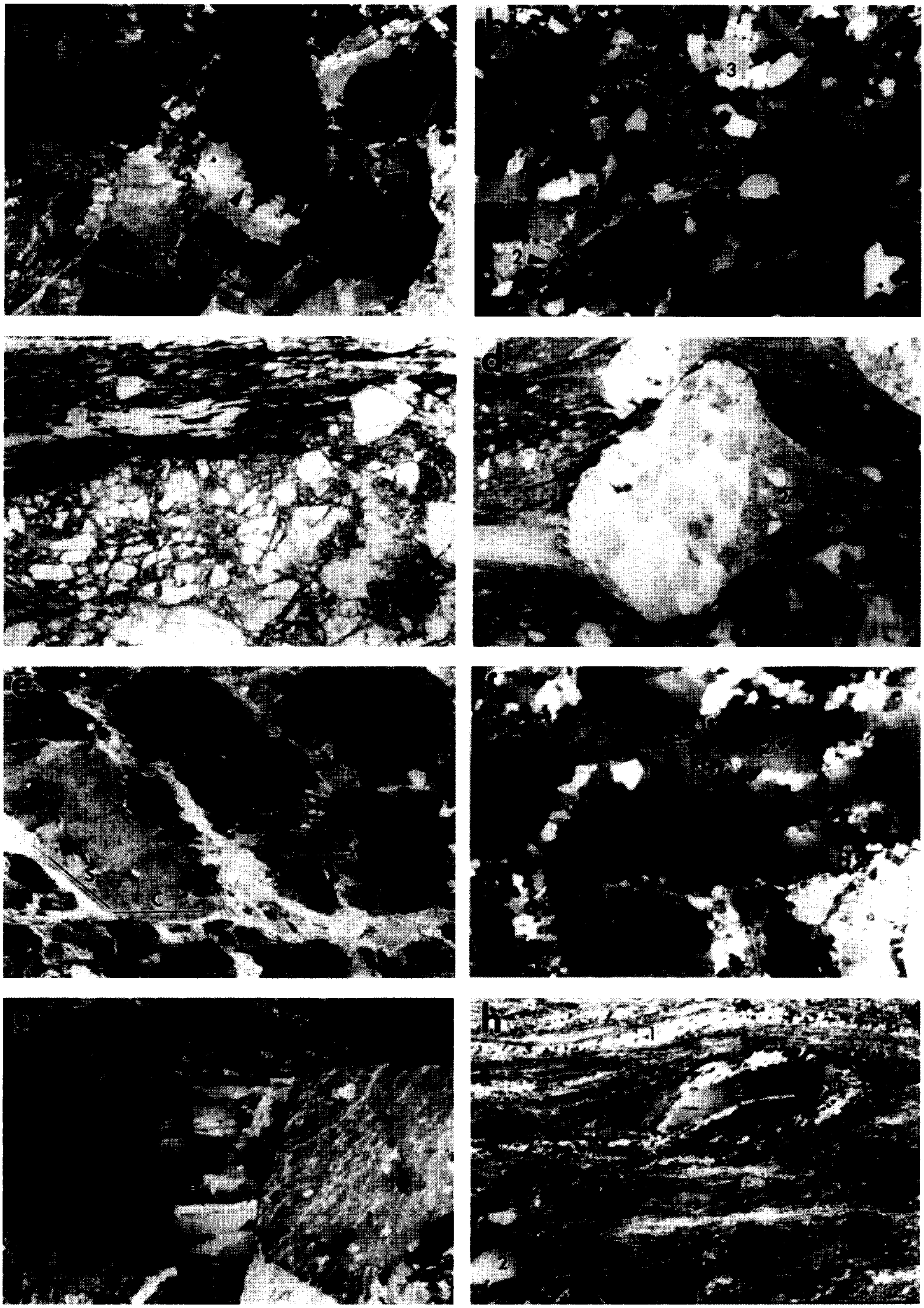

role during the early stages of plastic deformation of the granite. Quartz I is slightly flattened and shows undulose extinction, subgrains and fracturing, but recrystallization is very incipient at this stage (Fig. 6f). In quartz, the fractures are either filled by heteroblastic aggregates of quartz or are partly healed and decorated by trails of fluid or solid (carbonate) inclusions. K-feldspar is microboudinaged and locally dissected by microshear zones. Fractures between fragments are filled with aggregates of equant to fibrous quartz + carbonate ($\pm$albite, chlorite and biotite) (Fig. 5g), and microshear zones are outlined by ultrafine-grained aggregates of albite. At the same time, K-feldspar is replaced by epitaxial albite along grain boundaries and microcracks, and commonly shows stress-induced flame perthites (Fig. 6g).

The volume of strain-supporting matrix progressively increases with strain through the complete replacement of the magmatic plagioclase and the involvement of fine-grained aggregates formed at dilational sites (microfractures and pressure shadows) or along microshear zones. The strongly monoclinal *S–C* foliation pattern of protomylonites gives way to more symmetric fabrics in mylonites. Grain size is further reduced by combined cataclasis and recrystallization. Dynamic recrystallization of quartz I becomes important. Most quartz I is replaced by dynamically recrystallized quartz II aggregates, characterized by a homogeneous grain size, a strong crystallographic and often shape fabrics, and is deformed into high aspect ratio lenses or layers elongated in the foliation (Fig. 6h). However, quartz I porphyroclasts may persist up to high strains in mica-rich mylonites. Other quartz aggregates in mylonites are derived from deformation of those aggregates formed by deposition at dilational sites. In mylonites, albite-rich lenticular domains and layers are derived from recrystallization and deformation of the albite pseudomorphs after K-feldspar.

The product of intense deformation are phyllonitic mylonites consisting of quartz, albite, white mica, biotite $\pm$ epidote. A fine layering is often present due to the alternation of quartz-rich, albite-rich or mica-rich layers. These rocks are free of relicts of magmatic minerals and have a well-developed planar foliation, locally deformed by extensional crenulation cleavages.

DISCUSSION

The Mont Blanc granites, over the whole studied area, show both brittle and plastic structures, in accordance with Baggio's description (Baggio, 1958). Our field data allow the different structures to be ordered in a relative chronological sequence. Joints and veins are the earliest tectonic structures. Joints affect undeformed granites, never pass through cataclasites, and are absent in mylonites and foliated granites. Veins never intrude cataclastic shear zones or mylonites. They are offset by cataclasites and, in mylonites, are deformed and rotated parallel to the shear planes undergoing folding, boudinage and recrystallization. In mylonites, lenses of relatively undeformed coarse-grained quartz-adularia veins are wrapped around by the mylonitic foliation and are likely derived from veins sliced off by former cataclastic deformation. The absence of veins cross-cutting the mylonitic foliation, at all stages of mylonite evolution, excludes the possibility that veins formed synkinematically in the mylonites and were deformed during incremental strain. Cataclasites and fault breccias are reactivated as plastic shear zones and never contain clasts of mylonites or foliated granite. In contrast, lenses of cataclasites or cataclastically deformed granites are included in mylonites. The overall structural picture represents a straightforward mesoscopic example of a brittle-to-plastic deformation and this is also well supported by microstructural observations. The domainal partitioning of the structural distribution, as shown in Fig. 2(a), may therefore represent an increasing strain sequence, or different time steps in the deformation evolution of the granite.

Brittle and plastic deformation elements show a geometric and/or kinematic correlation. Veins are systematically oriented in the shortening domain relative to the shear displacement, and sigmoidal veins give a kinematic indication consistent with the shear displacement inferred in cataclasites and mylonites. Veins and joints are arranged in two sets and within each set they are mutually perpendicular. The correlation is even more evident than in Fig. 2 if each single joint–vein couple is considered. This indicates a genetic rather than an overprinting relationship and could suggest that brittle

Fig. 6. Microstructures in deformed Mont Blanc granites. (a) Aggregates of dominant quartz (arrows) along grain-boundary and transgranular fractures in 'undeformed' granites. (b) Sets of microfractures with different orientation, in incipient cataclastic shear zones, filled with dominant white mica (1 and 2) and quartz (3). Fracture (1) is parallel to the shear plane and the sense of shear displacement dextral. (c) Well-preserved tectonic microbreccia (lower part of the photo) including angular fragments of granite set in a dark structureless matrix. In the upper part of the photo, the microbreccia is foliated due to plastic deformation. (d) Porphyroclast of fine-grained granite inside a ductilely deformed fault breccia (white domains are quartz, and grey domains are sericitized plagioclase). In the matrix, the foliation is outlined by strongly oriented white mica and biotite forms tails around the porphyroclasts (1). Relics of the isotropic cataclastic matrix have been locally shielded from ductile deformation in the regions around porphyroclasts (2). (e) *S–C* composite foliation outlined by reaction-softened thin layers of white-mica along plagioclase grain-boundaries and microfractures. (f) Deformation microstructures of magmatic quartz in a protomylonite including microfractures (1), filled with quartz II aggregates, wavy extinction, subgrain poligonization (e.g. 2) and incipent recrystallization (e.g. 3). (g) V-pull-apart in a K-feldspar porphyroclast filled with fibrous quartz + carbonate. In the K-feldspar, epitaxial albite (lighter zones in the porphyroclast) occurs along a dense network of stress-induced flame perthites and thin microfractures. (h) Ribbons of fine-grained quartz II aggregates (1), derived from dynamic recrystallization of magmatic quartz, and partly recrystallized quartz I porphyroclasts (2) in a mylonite. Other porphyroclasts in the mica-rich schistose matrix (e.g. 3) are K-feldspar. (a), (b), (e), (f), (g) and (h): crossed polars; (c) and (d): plane light. The base of the photo is 3.25 mm in (c) and (f), and is 6.5 mm in (a), (b), (d), (e), (g) and (h).

and ductile structures are the result of a progressive incremental deformation rather than two distinct deformation phases. However, the relative geometric arrangements of joints, veins and cataclasites does not fit into a simple model since we do not have an explanation for the presence of two sets of joints and veins.

Plastic deformation has occurred under greenschist facies metamorphic conditions and has preferentially developed in zones that have previously undergone brittle deformation. We have no clear-cut evidence to decide whether the brittle-to-plastic transition has occurred as a result of an increase of temperature, decrease in strain rate, infiltration of fluids and related alteration of granites, grain-size reduction by cataclasis or a combination of these factors. It is, however, clear that textural and mineralogical changes geometrically associated with brittle structures (either 'coeval' or due to different deformation regimes) have a main role in localizing the plastic deformation. It is beyond the scope of this paper to discuss in detail the softening effects of the above factors, which has been dealt with extensively in several papers (e.g. Mitra, 1984; Simpson, 1986; Evans, 1990; Tourigny and Tremblay, 1997).

The structural evolution recorded in the Mont Blanc is a deformation sequence that most rocks originally at shallow levels are likely to have suffered when deformed along a prograde path during tectonic burial. However, brittle-to-plastic structural associations rarely occur in rocks, and this can probably be attributed to the metastable nature of brittle fabrics under metamorphic conditions, where they can easily be reactivated or even completely erased with increasing strain. The structures of the Mont Blanc represent a rather exceptional example of demonstrable brittle-to-ductile deformation. Brittle structures, including an association of joints, veins and cataclastic shear zones, are well preserved at all scales, and all stages of ductile overprinting are recorded. Thus, the Mont Blanc granites provide a key to understanding the control of early brittle fabric on subsequent plastic deformation and may explain features of the bulk deformation patterns in mylonites. In the study case, the following features of plastic structures may be recognized as developing as a consequence of the brittle-to-plastic history: (1) strongly heterogeneous strain patterns, (2) high lateral continuity, (3) discontinuous-type of mylonites, (4) high intersection angles between mylonites, and (5) common occurrence of granite porphyroclasts in some mylonites.

Heterogeneous strain patterns

In the Mont Blanc granites, there is evidence that mylonites are localized in the cataclastic shear zones or in cataclasites and fault breccias. This may be explained by the strain softening induced by grain-size reduction by cataclasis, fluid infiltration and granite alteration along the brittle discontinuities. Thus, brittle structures may provide secondary rheological discontinuities in otherwise homogeneous rocks. Plastic deformation focuses on these weaker zones, without (or only slightly) affecting the surrounding granite. The close spatial correlation between brittle and plastic shear zones is supported by the fact that the thickness of mylonites is in the same range as that of cataclasitic shear zones.

High lateral continuity of shear zones

Mylonites have often the high lateral continuity which is typical of faults. In some cases, a narrow (less than one metre wide) shear zone may be traced for hundreds of metres or even kilometres.

Discontinuous plastic shear zones

In the Mont Blanc granites, continuous shear zones, characterized by sigmoidal foliations, are rare (and limited to some minor shear zones in foliated granites) or absent. Almost all plastic shear zones are discontinuous, with foliation parallel to the shear zone boundary sharply in contact with 'undeformed' granite. Sharp contacts between shear zones and almost undeformed protoliths have already been recognized as inherited structures of initial cataclasis (e.g. Goodwin and Wenk, 1995). In fact, a very high strain gradient can be easily explained by the strong differences in rheological properties induced by the brittle deformation.

High angles between intersecting mylonites

Since mylonites nucleate on brittle structures, it is also clear that the spatial distribution of the early brittle discontinuities controls the pattern of mylonites. The anastomosing geometry of plastic shear zones is inherited from the pre-existing conjugate arrangement of cataclastic shear zones and from the intersecting directions of previous veins and joint sets. Veins may influence the pattern of cataclastic shear zones, which are seen to deviate in the direction of major veins. In granites, anastomosing patterns of plastic shear zones are commonly characterized by low intersection angles, generally in the range of 25–45° (Ramsay, 1980), giving rise to typical lens-shaped, low strain domains. In the Mont Blanc granites, mylonites commonly intersect at angles less than 30°, but locally preserve orientations and intersection angles greater than 45° similar to those of cataclastic shear zones in domains with dominant brittle deformation; narrow mylonites may locally show intersection angles higher than 80°. High intersection angles, in some cases close to orthogonal, may be seen in mylonites inferred to have developed on pre-existing brittle structures (e.g. Tobisch *et al.*, 1991; Tourigny and Tremblay, 1997). In the Mont Blanc granites, there is evidence that intersection angles between mylonites are progressively reduced, with increasing strain, by some plastic deformation in the intervening pods (where granites are transformed to foliated gneiss) and the mylonites rotate towards the bulk flow plane [see also the deformation steps during progressive deformation reported by Tobisch *et al.* (1991)].

Mylonites including granite porphyroclasts

A particular mylonite type develops during the plastic overprint of fault breccias. It consists of a mylonite including abundant, rounded porphyroclasts of granite derived from breccia clasts. During plastic reactivation of a fault, deformation concentrates on the fine-grained cataclastic matrix, which develops a foliation, and clasts may remain resistant up to high strain only undergoing some rounding. Deformation partitioning during mylonitization of a granite may isolate pods of relatively undeformed granite in a mylonite, but these pods are commonly lens-shaped and do not form a main fabric element of the mylonites as in deformed breccias.

There is not, of course, a one-to-one correspondence between the above mylonite features and the presence of a precursor brittle deformation. Heterogeneous strain fabrics are commonly formed by solely plastic deformation, and discontinuous shear zones are produced by evolution of continuous shear zones during increasing strain. However, in areas where the plastic shear zones have been inferred to nucleate on previous brittle structures, mylonites display most or all of the characteristics found in the Mont Blanc granites. For example, Tourigny and Tremblay (1997) have recognized a brittle-to-ductile evolution in the granites of the Abitibi Belt in Canada. They describe the occurrence of mainly discontinuos shear zones and report very high angles between mylonites. Strikingly similar features may be seen in mylonites described in granodiorites from the Santa Rosa mylonite zone in California (Goodwin and Wenk, 1995). We suggest that the combined occurrence of most or all the above-mentioned features in deformed granites may be a reliable criterion for recognizing (or at least suspecting) the existence of a brittle precursor where direct evidence has been lost by complete plastic overprinting of the brittle fabrics with the progression of deformation.

Gapais *et al.* (1987) have suggested that the three-dimensional array of shear zones through isotropic rocks, such as granites, may be used to estimate the bulk finite strain ellipsoid and aspects of the bulk deformation history. In the Mont Blanc area, there are indications that the patterns of plastic deformation are deeply dependent, in cases of a brittle-to-ductile evolution, on the geometric arrangement of the precursor brittle structures. The control of brittle structures on developing mylonites is strong in the initial stages and is progressively reduced and eventually lost as deformation proceeds. As plastic deformation increases and involves the intervening low strain domains between mylonites, the mylonite pattern may gradually equilibrate to the imposed bulk kinematic framework. However, in cases of narrow shear zones across undeformed rocks, especially those having characteristics described above for the Mont Blanc mylonites, the inferences of kinematic parameters from the shear zone geometries may be misleading.

CONCLUSIONS

Deformation in the Mont Blanc granites represents a well-preserved example of a macroscopic brittle-to-plastic deformation history. From the geometric point of view, the following sequence of structures may be recognized: (1) joints and veins; (2) cataclasites; (3) mylonites and foliated granites. The presence of a macroscopic brittle precursor has a strong influence on the way in which the following plastic deformation develops and results in: (1) strong localization of plastic strain; (2) high lateral continuity of mylonitic horizons; (3) sharply bounded discontinuous plastic shear zones; (4) high intersection angles between mylonites; and (5) mylonites with granite porphyroclasts.

The preservation of all the brittle-to-plastic deformation stages, as in the Mont Blanc granites, is rather uncommon, owing to the poor preservation of brittle fabrics under higher grade or prolonged metamorphic conditions. However, even where a complete plastic reactivation and overprint of brittle structures have occurred, the above features are usually maintained and may record the existence of a precursor brittle episode in isotropic rocks. If mylonites inherit the former orientations of brittle discontinuities, caution must be exercised when attempting to relate the geometric pattern of plastic shear zones to the bulk kinematic framework.

Acknowledgements—This work was in part supported by grants from M.U.R.S.T. 60% (G.V. Dal Piaz) and C.N.R. (Centro di Studio per la Geodinamica Alpina). We wish to thank G. V. Dal Piaz, for reading an early version of the manuscript, and J. Evans, N. Mancktelow and an anonymous referee for review. We also acknowledge A. Phillips for having improved our English.

REFERENCES

Andersen, T., Austrheim, H. and Burke, E. A. J. (1991) Fluid-induced retrogression of granulites in the Bergen Arcs, Caledonides of W. Norway: Fluid inclusion evidence from amphibolite-facies shear zones. *Lithos* **27**, 29–42.

Antoine, P., Pairis, J.-L. and Pairis, B. (1975) Quelques observation nouvelles sur la structure de la couverture sédimentaire interne du massif du Mont-Blanc, entre le Col du Ferret (frontière italo–suisse) et la Tête des Fours (Savoie, France). *Géologie Alpine* **51**, 5–23.

Baggio, P. (1958) Il granito del Monte Bianco e le sue mineralizzazioni uranifere. *Studi e ricerche della divisione geomineraria CNRN, Roma* **1**, 1–130.

Baggio, P. (1964) Contributo alla conoscenza geologica del versante italiano del Monte Bianco. *Atti dell'Istituto Veneto di Scienze Lettere ed Arti* **122**, 293–325.

Baggio, P., Ferrara, G. and Malaroda, R. (1967) Results of some Rb/Sr age determinations of the rocks of the Mont Blanc tunnel. *Bollettino della Società Geologica Italiana* **86**, 193–212.

Baggio, P. and Mezzacasa, G. (1971) Carta geologica della zona tra la Brenva e T.^{re} Jetoula (Massiccio del Monte Bianco). *S.T.E.M. Mucchi*, Modena.

Belliere, J. (1988) On the age of mylonites within the Mont Blanc massif. *Geodinamica Acta* **2**, 13–16.

Bertini, G., Marcucci, M., Nevini, R., Passerini, P. and Sguazzoni, G. (1985) Patterns of faulting in the Mont Blanc granite. *Tectonophysics* **111**, 65–106.

Bonin, B., Brändlein, P., Bussy, F., Desmons, J., Eggenberger, U., Finger, F., Graf, K., Marro, Ch., Mercolli, I., Oberhänsli, R., Ploquin, A., von Quadt, A., von Raumer, J., Schaltegger, U., Steyrer, H. P., Visonà, D. and Vivier, G. (1993) Late Varisican Magmatic Evolution of the Alpine Basement. In *Pre-Mesozoic Geology in the Alps*, eds J. F. von Raumer and F. Neubauer, pp. 171–201. Springer, Heidelberg.

Borghi, A., Gallo, L. M. and Porro, A. (1987) Osservazioni petrografiche nel settore francese del traforo del Monte Bianco. *Bollettino del Museo Regionale di Scienze naturali di Torino* **5**, 69–96.

Boundy, T. M., Fountain, D. M. and Austrheim, H. (1992) Structural development and petrofabric of eclogite facies shear zones, Bergen Arcs, western Norway: implications for deep crustal deformation processes. *Journal of Metamorphic Geology* **10**, 127–146.

Bürgmann, R. and Pollard, D. D. (1994) Strain accommodation about strike-slip fault discontinuities in granitic rocks under brittle-to-ductile conditions. *Journal of Structural Geology* **16**, 1655–1674.

Bussy, F., Schaltegger, U. and Marro, C. (1989) The age of the Mont-Blanc granite (Western Alps): a heterogeneous system dated by Rb Sr whole rock determinations on its microgranular enclaves. *Schweizerische mineralogische und petrographische Mitteilungen* **69**, 3–13.

Butler, R. W. H. (1985) The restoration of thrust systems and displacement continuity around the Mont Blanc massif, NW external Alpine thrust belt. *Journal of Structural Geology* **7**, 569–582.

Escher, A., Masson, H. and Steck, A. (1993) Nappe geometry in the Western Swiss Alps. *Journal of Structural Geology* **15**, 501–509.

Evans, J. P. (1990) Textures, deformation mechanisms, and the role of fluids in the cataclastic deformation of granitic rocks. In *Deformation Mechanisms, Rheology and Tectonics*, eds R. J. Knipe and E. H. Rutter, pp. 29–39. Geological Society Special Publication **54**.

Früh-Green, G. L. (1994) Interdependence of deformation, fluid infiltration and reaction progress recorded in eclogitic metagranitoids (Sesia Zone, Western Alps). *Journal of Metamorphic Geology* **12**, 327–343.

Gapais, D., Bale, P., Choukroune, P., Cobbold, P. R., Mahjoub, Y. and Marquer, D. (1987) Bulk kinematics from shear zone patterns: some field examples. *Journal of Structural Geology* **9**, 635–646.

Gaudemer, Y. and Tapponnier, P. (1987) Ductile and brittle deformations in the northern Snake Range, Nevada. *Journal of Structural Geology* **9**, 159–180.

Gibson, R. G. (1990) Nucleation and growth of retrograde shear zones: an example from the Needle Mountains, Colorado, U.S.A. *Journal of Structural Geology* **12**, 339–350.

Gibson, R. G. and Gray, D. R. (1985) Ductile-to-brittle transition in shear during thrust sheet emplacement, Southern Appalachian thrust belt. *Journal of Structural Geology* **7**, 513–525.

Goodwin, L. B. and Wenk, H.-R. (1995) Development of phyllonite from granodiorite: Mechanisms of grain-size reduction in the Santa Rosa mylonite zone, California. *Journal of Structural Geology* **17**, 689–707.

Guermani, A. (1997) La deformazione nei graniti: l'esempio del Monte Bianco. Tesi di dottorato, Padova.

Hobbs, B. E., Ord, A. and Teyssier, C. (1986) Earthquakes in the ductile regime? *Pure and Applied Geophysics* **124**, 309–336.

Kronenberg, A. K., Segall, P. and Wolf, G. H. (1990) Hydrolytic weakening and penetrative deformation within a natural shear zone. *American Geophysical Union Monographic Series* **56**, 21–36.

Leutwein, F., Poty, B., Sonet, J. and Zimmermann, J. L. (1970) Age des cavités à cristaux du granite du Mont Blanc. *Comptes Rendus de l'Académie des Sciences Paris* **271**, 156–158.

Macaudiere, J. and Brown, W. L. (1982) Transcrystalline shear fracturing and pseudotachylite generation in a meta-anorthosite (Harris, Scotland). *Journal of Structural Geology* **4**, 395–406.

McNulty, B. A. (1995) Pseudotachylyte generated in the semi-brittle and brittle regimes, Bench Canyon shear zone, central Sierra Nevada. *Journal of Structural Geology* **17**, 1507–1521.

Marro, C. (1987) Histoire des granitoides du Mont Blanc en Suisse. *Bulletin de la Société de Fribourg des Sciences Naturelles* **76**, 73–128.

Means, W. D. (1989) Synkinematic microscopy of transparent polycrystals. *Journal of Structural Geology* **11**, 163–174.

Mitra, G. (1984) Brittle to ductile transition due to large strains along the White Rock thrust, Wind River mountains, Wyoming. *Journal of Structural Geology* **6**, 51–61.

Passchier, C. W. (1982) Pseudotachylyte and the development of ultramylonite bands in the Saint-Barthélemy Massif, French Pyrenees. *Journal of Structural Geology* **4**, 69–79.

Pennacchioni, G. (1996) Progressive eclogitization under fluid-present conditions of pre-Alpine mafic granulites in the Austrolalpine Mt Emilius Klippe (Italian Western Alps). *Journal of Structural Geology* **18**, 549–561.

Pennacchioni, G. and Cesare, B. (1997) Ductile–brittle transition in pre-Alpine amphibolite facies mylonites during evolution from water-present to water-deficient conditions (Mont Mary nappe, Italian western Alps). *Journal of Metamorphic Geology* **15**, 777–791.

Poty, B. P., Stalder, H. A. and Weisbrod, A. M. (1974) Fluid inclusion studies in quartz from fissures of Western and Central Alps. *Schweizerische mineralogische und petrographische Mitteilungen* **54**, 717–752.

von Raumer, J. F. (1967) Kristallization und Gefügebildung im Mont Blanc-Granit. *Schweizerische mineralogische und petrographische Mitteilungen* **47**, 499–579.

von Raumer, J. F. (1974) Zur Metamorphose amphibolitischer Gesteine im Altkristallin des Mont Blanc- und Aiguilles-Rouges-Massivs. *Schweizerische mineralogische und petrographische Mitteilungen* **54**, 471–488.

von Raumer, J. F., Menot, R. P., Abrecht, J. and Biino, G. (1993) The Pre-Alpine Evolution of the External Massifs. In *Pre-Mesozoic Geology in the Alps*, eds J. F. von Raumer and F. Neubauer, pp. 221–240. Springer, Heidelberg.

Ramsay, J. R. (1980) Shear zone geometry: a review. *Journal of Structural Geology* **2**, 83–99.

Rubie, D. C. (1986) The catalysis of mineral reactions by water and restrictions on the presence of aqueous fluid during metamorphism. *Mineralogical Magazine* **50**, 399–415.

Rutter, E. H. (1986) On the nomenclature of the mode of failure transition in rocks. *Tectonophysics* **122**, 381–387.

Segall, P. and Simpson, C. (1986) Nucleation of ductile shear zones on dilatant fractures. *Geology* **14**, 56–59.

Sibson, R. H. (1977) Fault rocks and fault mechanisms. *Journal of the Geological Society of London* **133**, 191–213.

Simpson, C. (1986) Fabric development in brittle-to-ductile shear zones. *Pure and Applied Geophysics* **124**, 269–288.

Tobisch, O. T., Barton, M. D., Vernon, R. H. and Paterson, S. R. (1991) Fluid-enhanced deformation: transformation of granitoids to banded mylonites, western Sierra Nevada, California, and southeastern Australia. *Journal of Structural Geology* **13**, 1137–1156.

Tourigny, G. and Tremblay, A. (1997) Origin and incremental evolution of brittle/ductile shear zones in granitic rocks: natural examples from the southern Abitibi Belt, Canada. *Journal of Structural Geology* **19**, 15–27.

Tullis, J. and Yund, R. A. (1977) Experimental deformation of dry Westerly granite. *Journal of Geophysical Research* **82**, 5705–5718.

Tullis, J. and Yund, R. A. (1980) Hydrolytic weakening of experimentally deformed Westerly granite and Hale albite rock. *Journal of Structural Geology* **2**, 439–451.

Tullis, J., Dell'Angelo, L. and Yund, R. A. (1990) Ductile shear zones from brittle precursors in feldspathic rocks: the role of dynamic recrystallization. In *The Brittle–Ductile Transition in Rocks*, eds A. Duba, W. Durham, J. Handin and H. Wang, pp. 67–81. American Geophysical Union Geophysical Monograph **56**.

Watts, M. and Williams, G. D. (1979) Fault rocks as indicators of progressive shear deformation in Guingamp region, Brittany. *Journal of Structural Geology* **1**, 323–332.

Venera, Z. and von Raumer, J. (1995) Evolution of deformational structures in the Mont Blanc massif. *Terra abstract* (Supplement to Terra Nova).

Venera, Z. and von Raumer, J. (1996) The Alpine overprint in the Mont Blanc massif: mesoscopic and microstructural evidence. 13th Annual meeting of the Swiss Tectonic Studies Group, Geneva, 1 March 1996.